The *Caenorhabditis elegans* nonmuscle myosin genes *nmy-1* and *nmy-2* function as redundant components of the *let-502*/Rho-binding kinase and *mel-11*/myosin phosphatase pathway during embryonic morphogenesis

Alisa J. Piekny*, Jacque-Lynne F. Johnson, Gwendolyn D. Cham and Paul E. Mains†

Genes and Development Research Group and Department of Biochemistry and Molecular Biology, University of Calgary, 3330 Hospital Dr NW, Calgary, AB, Canada, T2N 4N1

*Present address: Research Institute of Molecular Pathology, Dr Bohr-Gasse 7, A-1030, Vienna, Austria
†Author for correspondence (e-mail: mains@ucalgary.ca)

Accepted 20 August 2003

Development 130, 5695-5704

doi:10.1242/dev.00807

Summary

Rho-binding kinase and the myosin phosphatase targeting subunit regulate nonmuscle contractile events in higher eukaryotes. Genetic evidence indicates that the *C. elegans* homologs regulate embryonic morphogenesis by controlling the actin-mediated epidermal cell shape changes that transform the spherical embryo into a long, thin worm. LET-502/Rho-binding kinase triggers elongation while MEL-11/myosin phosphatase targeting subunit inhibits this contractile event. We describe mutations in the nonmuscle myosin heavy chain gene *nmy-1* that were isolated as suppressors of the *mel-11* hypercontraction phenotype. However, a *nmy-1* null allele displays elongation defects less severe than mutations in *let-502* or in the single nonmuscle myosin light chain gene *mlc-4*. This results because *nmy-1* is partially redundant with another nonmuscle myosin heavy chain, *nmy-2*, which was previously known only for its role in anterior/posterior polarity and cytokinesis in the early embryo. At the onset of elongation, NMY-1 forms filamentous-like structures similar to actin, and LET-502 is interspersed with these structures, where it may trigger contraction. MEL-11, which inhibits elongation, is initially cytoplasmic. In response to LET-502 activity, MEL-11 becomes sequestered away from the contractile apparatus, to the plasma membrane, when elongation commences. Upon completion of morphogenesis, MEL-11 again appears in the cytoplasm where it may halt actin/myosin contraction.

Supplemental data available online

Key words: *C. elegans*, Rho-binding kinase, Myosin phosphatase, Nonmuscle myosin, Morphogenesis

Introduction

Morphogenesis transforms the *C. elegans* embryo from a roughly spherical ball into a long, thin worm. In contrast to most other animal systems, *C. elegans* morphogenesis occurs in the absence of widespread cell growth, proliferation or movements (reviewed by Chin-Sang and Chisholm, 2000; Simske and Hardin, 2001). Embryonic elongation occurs when actin filaments within a subset of epidermal cells (the lateral epidermal or 'seam' cells) shorten, causing the cells, and the embryo, to lengthen. Actin is initially disorganized within the lateral epidermal cells; however, at the onset of elongation, actin organizes into filaments that shorten as elongation proceeds (Priess and Hirsh, 1986).

let-502/Rho-binding kinase (ROK) and *mel-11*/myosin phosphatase targeting subunit (MYPT or myosin-binding subunit MBS) regulate the cell shape changes within the lateral epidermal cells to drive elongation. Based on genetic data coupled with the known functions of their vertebrate homologs in the regulation of smooth muscle contraction and focal adhesions formation (Kaibuchi et al., 1999; Pfitzer, 2001; Piekny et al., 2000; Shelton et al., 1999; Somlyo and Somlyo, 2000; Wissmann et al., 1997), *let-502* and *mel-11* probably regulate elongation by altering the activity of myosin. Contraction is triggered by phosphorylation of regulatory myosin light chain (rMLC, *mlc-4* in *C. elegans*) by myosin light chain kinase or integrin-linked kinase (Pfitzer, 2001; Somlyo and Somlyo, 2000). Myosin phosphatase in turn removes the activating phosphate from rMLC, preventing contraction. Activation of ROK by the small GTPase Rho results in an inhibitory phosphorylation of the targeting subunit MYPT of myosin phosphatase, releasing the block to contraction. *let-502*/ROK and *mlc-4*/rMLC mutants fail to elongate, while *mel-11*/MYPT mutants hypercontract.

The *Drosophila* homologs Drok/ROK and MYPT similarly regulate morphogenetic processes. Nonmuscle MHC *zipper* and rMLC *spaghetti-squash*, Drok and Mypt/Dmbs are required for dorsal closure (Mizuno et al., 2002; Tan et al., 2003; Winter et al., 2001; Young et al., 1993). These molecules also are involved in other developmental processes such as epidermal planar polarization (Winter et al., 2001). Therefore, nonmuscle myosin, ROK and MYPT probably comprise a conserved 'cassette' that is used for many

developmentally-specific contractile processes during animal development.

To identify new components of the *C. elegans* elongation pathway, we screened for suppressors of the *mel-11* hypercontraction phenotype (Piekny et al., 2000). Here, we describe *nmy-1*, which encodes a nonmuscle myosin heavy chain (MHC). Genetic evidence is consistent with *nmy-1* acting as a partner for MLC-4/rMLC, the downstream target for LET-502/ROK and MEL-11/MYPT. However, the *nmy-1* null mutant phenotype is less severe than *mlc-4* or *let-502*, suggesting that *nmy-1* functions redundantly. Indeed, we found that *nmy-2*, previously known only for its requirement in the early embryo (Cuenca et al., 2003; Guo and Kemphues, 1996) acts in concert with *nmy-1*. In addition, NMY-1 antisera reveal that this protein forms filamentous-like structures in the lateral epidermal cells during elongation.

The expression pattern of LET-502 and MEL-11, determined by GFP transcriptional reporters, is consistent with their functioning as regulators of elongation (Wissmann et al., 1999). LET-502, the trigger for contraction, is expressed in the same lateral epidermal cells as MLC-4 that drive elongation (Shelton et al., 1999; Wissmann et al., 1999). MEL-11, the negative regulator of contraction, is also expressed within these cells; however, at lower levels than in the neighboring dorsal and ventral epidermal cells (Wissmann et al., 1999). A caveat is that these reporters revealed only zygotic transcription, although either maternal or zygotic activity of the two genes suffices for viability. Therefore we do not know precisely in which cells the genes act nor the mechanism by which LET-502 and MEL-11 regulate epidermal cell shape changes. For example, they could regulate myosin contraction and/or tether actin cables to the membrane during morphogenesis. Using antisera against LET-502 and MEL-11, we show that both proteins are expressed in the lateral epidermal cells during elongation. Although LET-502 localizes near myosin throughout elongation, MEL-11 becomes sequestered away from the contractile apparatus in response to LET-502 activity. Thus, LET-502 and MEL-11 act at the level of myosin contractility.

Materials and methods

Strains and alleles

C. elegans were maintained under standard conditions (Brenner, 1974). Strains were constructed using standard procedures, and cis-linked morphological markers were often used to follow the mutations used through crosses. Homozygous lethal or sterile mutations were maintained as heterozygous stocks balanced either with appropriate crossover suppressors or normal chromosomes with flanking morphological markers. To determine hatching rates of different genetic combinations, as many L4 hermaphrodites as needed were brooded at the appropriate temperatures until they ceased laying fertilized embryos; a minimum of 300 progeny were scored unless otherwise noted (Mains et al., 1990).

Nomenclature follows that of Horvitz et al. (Horvitz et al., 1979). Genes, alleles and balancer chromosomes listed are below; descriptions can be found in Edgley et al. (Edgley et al., 1995), Hodgkin (Hodgkin, 1997) and in Wormbase (www.wormbase.org).

Linkage Group I: *let-502*(*ca201*, *sb106*ts and *sb108*), *dpy-5(e61)*, *rde-2(ne221)*. Linkage Group II: *mel-11*(*it26*ts and *sb55*), *unc-4(e120)*, *sqt-1(sc13)*. Linkage Group III: *mlc-4(or253)*. Linkage Group V: *sma-1(e30)*. Linkage Group X: *unc-115(e2225)*, *dpy-8(e130)*, *unc-78(e1217)*, *spc-1(ra409)*, *nmy-1*(*sb92*, *sb113* and *sb115*), *unc-2(e55)*. Balancer chromosomes: the crossover suppressor *mnC1 II* was used to balance *mel-11*.

Single nucleotide polymorphism mapping

Single nucleotide polymorphism mapping was performed as described by Wicks et al. (Wicks et al., 2001). The Dumpy (Dpy) and Lumpy phenotype of *sb113* was mapped to the left arm of LG*X* by crossing with the Hawaiian strain CB4856 and using primers indicated in Wicks et al. (Wicks et al., 2001). Another mutant, *sb115*, was mapped to the left arm of LG*X* between *dpy-8* and *unc-115* via classical genetics. *sb92* has no phenotype on its own but was mapped between *unc-2* and *unc-78* based on suppression of *mel-11*. *sb115 dpy-8* was crossed to CB4856, and Lumpy non-Dpy and Dpy non-Lumpy recombinants were selected, mapping *sb115* between polymorphisms Y41G9A and F52E4 (data submitted to Wormbase). Cosmid F52B10 is within this region and contains *nmy-1*. Two independent PCR products spanning *nmy-1* in *sb92*, *sb113* and *sb115*, were sequenced (University of Calgary Core DNA Sequencing Laboratory) (Piekny et al., 2000) and were found to contain mutations (see Results).

Microscopy and immunofluorescence

Embryos were dissected from gravid hermaphrodites that had been incubated without food for 1 hour. This induces animals to hold their eggs, enriching for mid-stage embryos. Embryos were mounted in M9 solution (Horvitz and Sulston, 1980) or larva and adults were placed in anaesthetizing solution (0.1% tricaine, 0.01% tetramisole) on 3% agarose pads. Specimens were examined by Nomarski optics on a Zeiss Axioplan 2 microscope, and images were photographed using the Hamamatsu Orca ER digital camera and collected using Axiovision 3.0 for Windows NT.

For indirect immunofluorescence, mid-staged embryos were placed on polylysine-coated slides in M9. A cover slip was placed on each slide, and the embryos were frozen on dry ice for at least 30 minutes. The cover slips were cracked off, and slides were placed in –20°C methanol for 10 minutes, followed by 20 minutes in –20°C acetone, then rehydrated with 90% ethanol for 10 minutes at –20°C, 60% ethanol for 10 minutes at –20°C, then 30% ethanol for 10 minutes at room temperature. For actin and some NMY-1 staining, freeze-cracked slides were placed in a 3.7% formaldehyde solution (w/v) in 1× phosphate-buffered saline (PBS) at room temperature for 10 minutes and then placed in 1× PBS with 0.1% Tween-20 (PBT). For all methods, the slides were placed directly into 1×PBT for a minimum of 1 hour, then incubated with appropriate dilutions of antisera in PBT with 20% normal goat or donkey serum (Jackson Immunoresearch Laboratories). F-actin was stained with phalloidin-Alexa 488 (Molecular Probes; 10 μl/slide was placed into a tube and the methanol was evaporated overnight, then 1×PBT was added with 20% normal goat serum and other antisera if needed). Rabbit anti-NMY-2 polyclonal antibodies (Guo and Kemphues, 1996) were used at a 1:50 dilution, rabbit anti-MEL-11 polyclonal antibodies at 1:50 (Piekny et al., 2002), rat anti-LET-502 polyclonal antibodies at 1:50 (Piekny et al., 2002), rat anti-NMY-1 polyclonal antibodies (see below) at 1:200 and rabbit anti-NMY-1 polyclonal antibodies (see below) at 1:1000. All slides were incubated with primary antibodies for 1 hour to overnight at room temperature and washed three times with PBT. Anti-rat IgG conjugated to indocarbocyanine (Cy-3; Jackson Immunoresearch Laboratories) and anti-rabbit IgG conjugated to Alexa 488 (Molecular Probes) were used at a 1:100 dilution in PBT, and slides were incubated at room temperature for 1 hour. Slides were washed three times with PBT and soaked in 1 μg/ml DAPI (Roche) for 1 minute at room temperature, washed with PBT, then mounted with a drop of Slowfade Light Antifade solution (Molecular Probes). Images were collected using Axiovision 3.0 for Windows NT as stacks of 20×1 μm from a Zeiss Axioplan 2 microscope using a 63× oil objective with the Hamamatsu Orca ER digital camera. Stacks were digitally deconvolved using the

constrained iterative algorithm of Axiovision 3.0 for Windows NT. Superficial stacks corresponding to epidermal cells or internal stacks corresponding to the pharyngeal/intestinal region were analyzed with Adobe Photoshop version 4.0 for Windows.

RNA-mediated interference (RNAi)

Double-stranded RNA (dsRNA) was generated for *nmy-1* and *nmy-2*. The primers for *nmy-1* were made to the C-terminal region of the coding sequence (sequence identity <80% with *nmy-2*). The primers were: forward primer (including the T3 promoter) 5′AATTAACCCTCACTAAAGGGGCAACATCAACTGACGAG3′ and reverse primer (including the T7 promoter) 5′TAATACGACTCACTATAGGGAGCATCGAGAAGATCGTC3′. Primers for *nmy-2* similarly were made to the C-terminal portion of the coding sequence showing lower sequence homology to *nmy-1*. The primers were: forward primer (including the T3 promoter) 5′AATTAACCCTCACTAAAGGGGACGAGACTCGATGCTGA3′ and reverse primer (including the T7 promoter) 5′TAATACGACTCACTATAGGGATCTCTGGAGAGTGTCTC3′. dsRNA was made from the PCR products and used for soaking worms as described in Piekny and Mains (Piekny and Mains, 2002). dsRNA to *nmy-1*, *nmy-2* and both together were injected as described by Fire et al. (Fire et al., 1998) with concentrations varying from 10^{-6} μg/μl to 1 μg/μl for each gene. Some *nmy-2* RNAi experiments were performed using bacteria expressing dsRNA from the feeding library described by Fraser et al. (Fraser et al., 2000). L4 or young adult were cultured for 1-2 days until first broods were obtained and were passaged to plates seeded with normal *E. coli* for subsequent broods.

NMY-1 antisera

Rat polyclonal antibodies were generated using a GST-NMY-1 fusion encoding C-terminal region amino acids 941-1133, which was amplified using the following primers: forward (containing the *Bam*HI restriction site) 5′TACAGGATCCGAGAAACCGTCCGTGATCTC3′ and reverse (containing the *Eco*RI restriction site) 5′CGAGGAATTCCCTTGTCATTTCTGCCTTAT3′ and cloned directionally into the pGEX-3X vector (Pharmacia). Rat injections were performed as described previously (Piekny and Mains, 2002). Rabbit polyclonal antibodies were raised against a GST-NMY-1 fusion by the Peptide Group from Macromolecular Resources. All antisera were purified by subtracting against a glutathione-sepharose 4B column (Pharmacia). Western blot analysis showed that all of the antisera recognized a predominant band above 200 kDa (expected ~230 kDa) with gravid adult hermaphrodite extracts obtained by 1×PBS and with extracts further solubilized with 1 M NaCl, implying that pools of NMY-1 are both cytoplasmic and associated with the cytoskeleton (data not shown). The band was blocked by adding excess GST-NMY-1 to the antisera (data not shown) and immunostaining was not detectable in *nmy-1(sb115)* (data not shown but see results), which truncates the protein before the region used for immunization.

Results

Identification of a new component of the *let-502/mel-11* pathway

Previously we performed a screen for suppressors of *mel-11* to identify new genes in the *let-502/mel-11* pathway (Piekny et al., 2000). *sb92*, *sb113* and *sb115* are semi-dominant suppressors (Table 1) that failed to complement for Dpy, Lumpy and Roller (Rol) phenotypes (genetic properties will be described below). *sb115* was mapped near cosmid F52B10 (Materials and methods), which contains a single gene, *nmy-1*. As diagrammed in Fig. 1, *nmy-1* is predicted to encode a 1963 amino acid nonmuscle MHC, with an N-terminal SH3-like domain, a myosin motor head followed by a myosin coiled-coil tail. *sb92* included a Glu(285)Val mutation, *sb113* Gly(647)Glu and *sb115* Gln(480)stop. All are in highly conserved residues within the head domain (Fig. 1). The myosin head and tail are highly conserved between NMY-1 and the *Drosophila* nonmuscle MHC, Zipper, human MHCB and another *C. elegans* MHC, NMY-2 (Fig. 1; see Fig. S1 at http://dev.biologists.org/supplemental/) (Guo and Kemphues, 1996; Mansfield et al., 1996; Philips et al., 1995; Young et al., 1993). Overall, NMY-1 shares highest amino acid identity (48%) with *Drosophila* Zipper and human MHCB. NMY-1 shares 45% identity with *C. elegans* NMY-2, suggesting that they are paralogs.

RT-PCR revealed one predominant SL1-spliced transcript of ~6000 bp, similar to the predicted length of 6383 nucleotides (data not shown). Sequencing confirmed the predicted intron/exon structure of *nmy-1* found at Wormbase (www.wormbase.org). In addition, microarray data predicts that *nmy-1* is most highly expressed during embryogenesis (Hill et al., 2000).

Table 1. Genetic interactions between *nmy-1* and genes in the *let-502/mel-11* elongation pathway

	20°C		25°C	
Genotype	Hatching (%)	L1 arrest (% of hatched)*	Hatching (%)	L1 arrest (% of hatched)*
mel-11(it26)	4	–†	0	–
mel-11(it26); nmy-1(RNAi)	71	Range of arrest	–	–
mel-11(it26); nmy-1(sb92)/+	23	0	–	–
mel-11(it26); nmy-1(sb92)	68	0	–	–
mel-11(it26); nmy-1(sb113)/+	48	5	23	44
mel-11(it26); nmy-1(sb113)	75	62	64	84‡
mel-11(it26); nmy-1(sb115)/+	35	56	27	74
let-502(sb108)	100	0	92	0
let-502(sb108); nmy-1(sb115)	–	–	88	82
mel-11(it26); spc-1(ra409)/+	7	100	–	–
mel-11(sb55)	–	–	6	0
sma-1(e30)	–	–	95	7
mel-11(sb55); sma-1(e30)	–	–	94	86
mel-11(it26); sma-1(e30)	68	92	–	–

*The L1 arrest phenotype was like *mlc-4* shown in Fig. 2, and differed from the slow-growing L1-L3 Lumpy Dpy larva observed in *nmy-1* homozygotes alone.
†Not determined.
‡All non-arrested animals were Lumpy Dpy.

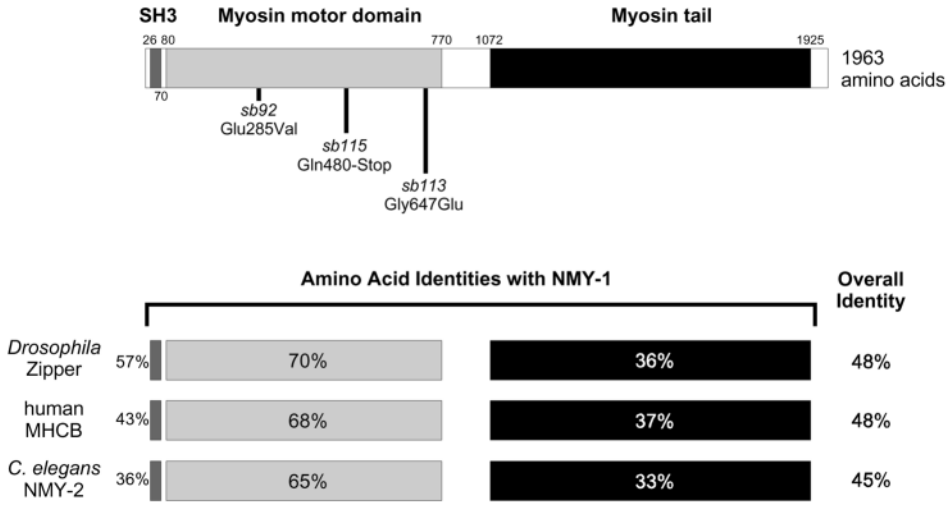

Fig. 1. Schematic representation of the predicted NMY-1 structure. The N terminus contains an SH3-like domain and a myosin motor domain, which contains the MLC binding sites (one for the regulatory MLC and one for the essential MLC). The C terminus includes a coiled-coil myosin tail domain, probably involved in MHC dimerization. *nmy-1* mutations are indicated. The overall amino acid identities between NMY-1 and *Drosophila* Zipper, human MHCB and *C. elegans* NMY-2 are shown as well as the identities between the SH3, myosin motor and myosin tail domains.

A previous large-scale RNAi survey reported sterility, lethality and Dpy and uncoordinated (Unc) phenotypes for *nmy-1* (Kamath et al., 2003). However, short regions of high DNA sequence identity to *nmy-2* in the myosin head domain could result in RNAi crossreactivity. We performed *nmy-1* gene-specific RNAi (Materials and methods) and observed little embryonic lethality but did see Dpy Lumpy phenotypes identical to those of our *nmy-1* alleles *sb113* and *sb115*. Like our *nmy-1* alleles, injection of *nmy-1* dsRNA suppressed *mel-11* lethality (Table 1).

nmy-1 alleles behave as semi-dominant suppressors of *mel-11* with stronger suppression when homozygous (Table 1). Although suppressed *mel-11; nmy-1* embryos hatch, a large proportion of the early larva with *sb113* and *sb115* arrested with an elongation phenotype similar to *let-502* and *mlc-4*. For example, 84% of *mel-11(it26)*; *nmy-1(sb113)* larva that hatched at 25°C displayed L1 arrest without elongation, in comparison to *nmy-1(sb113)* alone, which displayed 1-4% L1-L3 larva arrest/slow growth (Table 2). All escapers showed the *sb113* Dpy, Lumpy phenotype, indicating that *mel-11* did not reciprocally suppress the *nmy-1* morphological defects. All *mel-11(it26)*; *nmy-1(sb115)* larva displayed L1 arrest compared with 30% for *sb115* alone (data not shown).

Characterization of *nmy-1*

Our alleles of *nmy-1* are the first reported for this gene. *sb92* has no obvious phenotypes on its own, while *sb113* and *sb115* are Dpy Lumpy Rol with some embryonic lethality (Table 2). All *sb113* and *sb115* L1 larva display bulging at the anterior (Fig. 2A,D), which usually disappears as the animals grew. *sb113* had a small percentage (1-4%) of slow growth or larval arrested between L1-L3 while the value was 30% for *sb115*. *sb113* and *sb115* adults are Dpy, Lumpy and sometimes Rol, consistent with non-lethal elongation defects, and adult hermaphrodites have low brood sizes (Table 2). Larva and adults have small pharynxes (Fig. 2G,H) and possible intestinal defects as bacteria accumulate in their guts. In addition, the adults show varying degrees of Unc, although whether this is a secondary consequence of the elongation defects remains to be determined. Gonad arms sometimes fail to migrate correctly (e.g. fail to turn in the DV axis), but this is probably a secondary consequence of other elongation defects as the distal tip cell migration is normal in L4 larva (data not shown).

All of the *nmy-1* alleles behave as loss-of-function alleles. The phenotypes of *sb113* and *sb115* are unchanged when heterozygous with each other or a chromosomal deficiency of the region (data not shown). *sb92* is more severe in trans to

Table 2. The phenotypes, hatching rates and brood sizes of *nmy-1* alleles

		15°C		20°C		25°C	
Parental genotype	Progeny phenotypes	Hatching (%)	Average brood	Hatching (%)	Average brood	Hatching (%)	Average brood
sb113	Lumpy, Dpy, Rol*	91†	20	84†	32	89†	22
sb113 × +/+ male	Wild type	100	150	99	190	99	127
sb115	Lumpy, Dpy, Rol*	76‡	15§	80‡	12	74‡	13
sb115 × +/+ male	Wild type	99	187	99	168	99	156
sb92	Wild type	99	213	96	256	93	230
nmy-1(RNAi)¶	Lumpy, Dpy, Rol*	–**	–	95	–	–	–

*All L1 larva showed severe Lumpy Dpy phenotypes that often disappeared by adulthood. The adults showed a range of phenotypes including mild Lumpy Dpy, and Rol. Some were also Unc.

†Approximately 1-4% grew slowly or arrested between L1-L3.

‡Approximately 30% grew slowly or arrested between L1-L3.

§n=115. n>300 for all other table entries.

¶RNAi was performed by both soaking or injection. The second broods showed L1 larva with Lumpy Dpy phenotypes (similar to *sb113* and *sb115* homozygotes).

**Not determined.

either allele or the deficiency than when homozygous, indicating that it represents a partial loss-of-function. *sb115* is likely a null allele based on its phenotypes and molecular lesion (a truncation in the N-terminal myosin head domain). *sb113* and *sb115* phenotypes were rescued by crossing mutant hermaphrodites to wild-type males, indicating zygotic activity of the genes (Table 2). *sb115*/*sb92* and *sb113*/*sb92* hermaphrodites show more severe phenotypes when the stronger alleles are maternally inherited, indicating some maternal activity, even though the NMY-1 protein is not detected in early embryos (data not shown).

NMY-1 is redundant with NMY-2

Although NMY-1 is predicted to partner with MLC-4, *nmy-1(null)* is viable while the *mlc-4(null)* is lethal (Shelton et al., 1999); all *mlc-4* mutant larva arrest at L1 with failed elongation (Fig. 2B). This result implies that *nmy-1* is not the only myosin target of the *let-502/mel-11* pathway. NMY-2 is a nonmuscle MHC with high levels of sequence similarity to NMY-1 (Fig. 1) and has been characterized for its role in anterior/posterior polarity and cytokinesis using RNAi (Cuenca et al., 2003; Guo and Kemphues, 1996). Because RNAi results in early, lethal defects, the role of *nmy-2* in elongation has not been explored.

To determine if *nmy-2* could potentially function redundantly with *nmy-1*, we stained wild-type embryos with NMY-2 antisera to determine if the protein persists through elongation. NMY-2 expression levels decreased with time, but it is presented at low levels in all cells, including epidermal cells, until after the onset of elongation, and this pattern was not altered in *nmy-1* mutant (Fig. 3A-I).

To establish redundancy between *nmy-1* and *nmy-2*, we performed *nmy-2(RNAi)* in wild-type and *nmy-1* mutant worms. To avoid the block of *nmy-2(RNAi)* at the one-cell stage, we used feeding as the means of dsRNA delivery, which gradually eliminates gene function over several days, permitting us to examine *nmy-1* interactions. The broods on the first day after reaching adulthood displayed 52% embryonic viability (Table 3), indicating that *nmy-2* was incompletely eliminated. However, L1 arrest phenotypes were never observed. *nmy-2(RNAi); nmy-1(sb113 or sb115)* displayed the same level of embryonic lethality as *nmy-2(RNAi)* alone, but half of the hatching embryos showed L1 arrest similar to *mlc-4* (Fig. 2B,E,F; Table 3). Although we normally see low levels of L1-L3 slow growth/arrest in both *nmy-1(sb113)* and *nmy-1(sb115)* alone, the L1 arrest phenotype seen in the double mutants was much stronger and distinctly like that seen in *mlc-4* (and *let-502*). The enhancement of *nmy-1* elongation defects by *nmy-2* suggests redundancy. Finally, *rde-2(ne221)*, which shows partial resistance to RNAi (Tabara et al., 1999) and thus may bypass the early block, produced 13% embryos with failed elongation when grown on *nmy-2(RNAi)* bacteria compared with none when fed normal bacteria (Table 3).

As *nmy-1* and *let-502* both suppress *mel-11*, we expected to see enhancement between *nmy-1* and *let-502* (Piekny et al., 2000). *let-502(sb108)*, a weak loss-of-function allele, shows no larval arrest, while approximately one-third of *nmy-1(sb115)* do so. However, *let-502(sb108)*; *nmy-1(sb115)* showed 82% L1 arrested with failed elongation (Table 1). Similar results were seen with other *nmy-1* and *let-502* allelic combinations (data not shown). Therefore, loss of *nmy-1* (which results in a

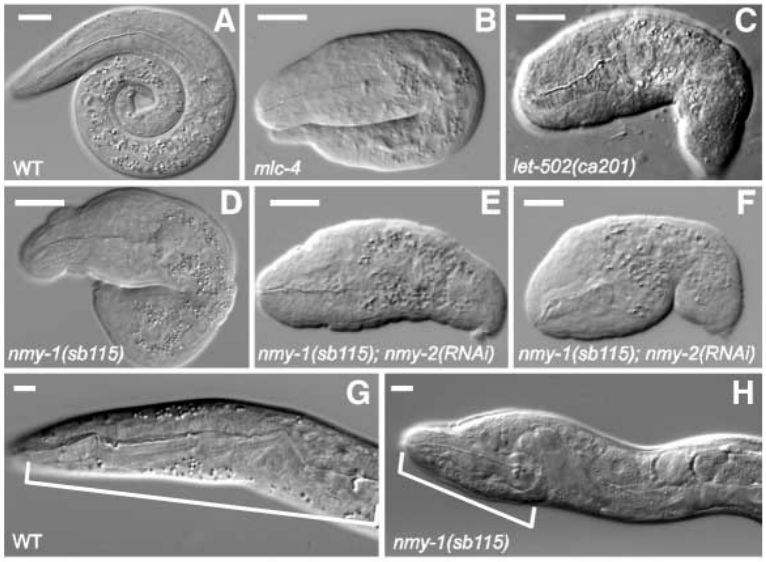

Fig. 2. Nomarski images of mutant L1 larva. (A) Wild type, (B) *mlc-4*, (C) *let-502(ca201)*, (D) *nmy-1(sb115)* and (E,F) *nmy-1(sb115); nmy-2(RNAi)*. (G,H) The adult pharynx of wild-type and *nmy-1(sb115)* hermaphrodite are indicated by brackets. Scale bars: 10 μm.

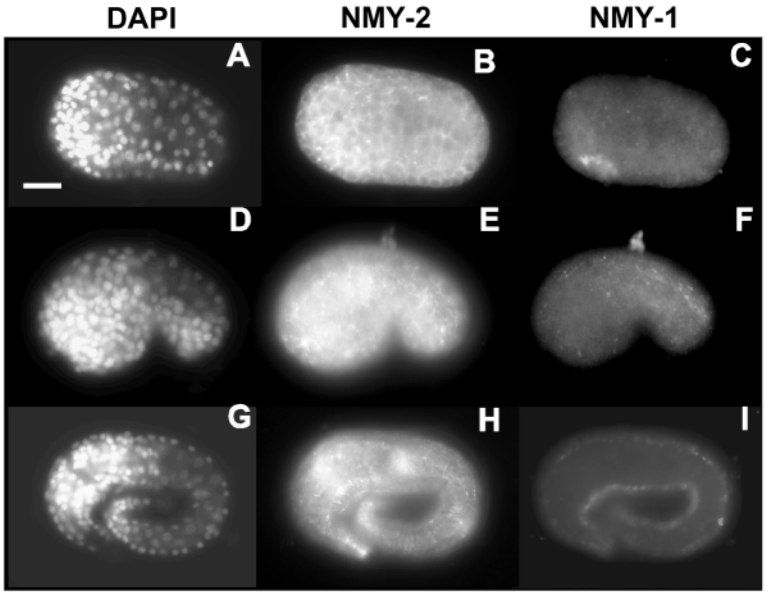

Fig. 3. NMY-1 and NMY-2 expression in *nmy-1(sb115)* mutant embryos. *nmy-1(sb115)* embryos were stained for DAPI (left column), NMY-2 (middle column) and NMY-1 (right column). NMY-2 was expressed prior (B), during (E) and after (H) elongation, although levels decreased. Anti-NMY-1 antisera failed to stain these embryos (C,F,I), with the exception of a low level of crossreactivity in muscle (I). Scale bar: 10 μm.

Table 3. Redundancy between *nmy-1* and *nmy-2* during elongation

Genotype*	Day one		Day two	
	Hatching (%)	L1 arrest† (% of hatched)	Hatching (%)	L1 arrest† (% of hatched)
nmy-2(RNAi)	52	0	0‡	–§
nmy-2(RNAi); nmy-1(sb113)	51	56	6	100
nmy-2(RNAi); nmy-1(sb115)	47¶	53	Ste	–
rde-2[f]	–	–	100	0
*nmy-2(RNAi); rde-2***	–	–	85	13

*RNAi was performed by feeding.
†The L1 arrest phenotype observed was a severe, Mlc-4-like arrest shown in Fig. 2B. This phenotype differed from the slow-growing L1-L3 Lumpy Dpy larva noted in Table 2.
‡n=117, all others values in the table are more than 190.
§Not determined.
¶n=109.
**Hermaphrodites were fed *nmy-2(RNAi)* for 1 day and were transferred to plates with normal bacteria for the day two brood.

partial loss of total NMY protein) synergizes with a partial loss of *let-502*, consistent with both acting in the same pathway.

NMY-1, LET-502 and MEL-11 localization during elongation

Our genetic results predict NMY-1 expression in the lateral epidermis during elongation. NMY-1 antisera revealed that it is indeed highly expressed in these cells at the onset of elongation (Fig. 4B), similar to that observed by Shelton et al. (Shelton et al., 1999) for MLC-4. NMY-1 was also present at the adherens junctions (AJs) of the developing pharynx (data not shown). As elongation proceeded, NMY-1 became more punctate (Fig. 4D) and organized into filamentous-like structures (Fig. 4F). Embryos of similar stages stained for actin showed a similar pattern, albeit filamentous structures become apparent earlier (Fig. 4A,C,E; embryos were not co-stained because NMY-1 and actin require incompatible fixation methods). Both actin and myosin organize into filaments that run perpendicular to the axis of elongation and are thus potentially arrayed to draw the lateral epidermal cells together in the dorsal/ventral axis, causing embryonic elongation.

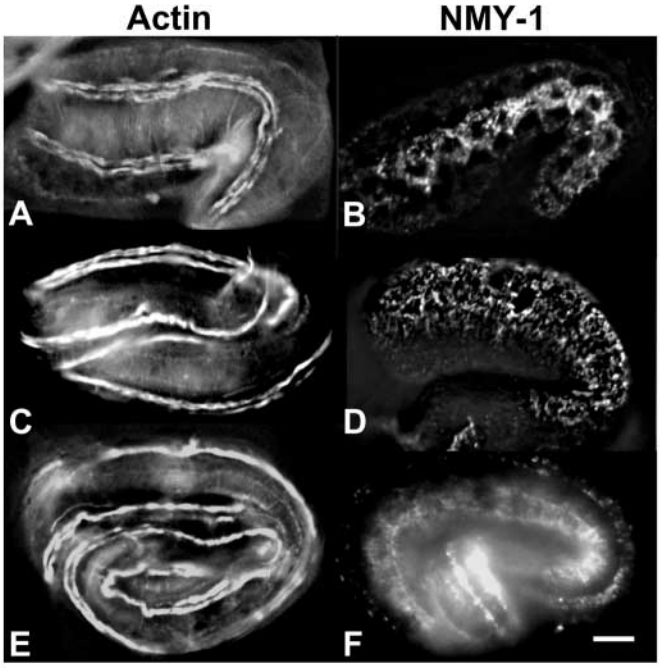

Fig. 4. NMY-1 and actin localization during elongation. Actin (A,C,E) and NMY-1 (B,D,F) localization are shown in deconvolved images of superficial sections of comparably-staged 1.5 to 3.0-fold wild-type embryos using immunofluorescence. Owing to incompatibilities with fixation methods for actin and NMY-1, we could not co-stain embryos. Scale bar: 10 μm.

The immunolocalization patterns of MEL-11 and LET-502 during morphogenesis is consistent with the hypothesis that they regulate the activity of myosin. Prior to elongation, LET-502 and MEL-11 showed extensive colocalization in the cytoplasm with punctate staining at epidermal cell boundaries (Fig. 5A-C). As elongation proceeded, MEL-11 became enriched and was restricted to cell boundaries while LET-502 remained primarily cytoplasmic (Fig. 5D-F). When elongation was completed, MEL-11 again increased in the cytoplasm, with decreased, punctate localization at cell boundaries, similar to the pre-elongation pattern (Fig. 5J-L). Both proteins were also expressed at the AJs of the developing pharynx and intestine (Fig. 5G-I) and in the germline precursor cells (data not shown).

These data suggest that LET-502, but not MEL-11, is in a region where it can influence contractions of actin/myosin filaments during elongation. Indeed, as elongation proceeded, punctate anti-LET-502 staining interspersed with the NMY-1 filaments (Fig. 6A-D). By contrast, MEL-11 was membrane bound, away from NMY-1 (Fig. 6E-H). The vertebrate MEL-11 homolog, MYPT, moves to the plasma membrane after phosphorylation by ROK, where it remains sequestered from actin/myosin to allow contraction (Shin et al., 2002). To determine if MEL-11 was similarly influenced by *let-502* activity, we examined MEL-11 localization in *let-502* mutants. Indeed, using the strong *let-502(ca201)* allele, MEL-11 remained mostly cytoplasmic with punctate cell membrane localization (Fig. 7A,B), similar to its distribution wild-type embryos prior to elongation (Fig. 5B). Because *let-502(ca201)* mutant embryos arrest at the onset of elongation, disrupted staining could arise as a secondary consequence of developmental arrest. Therefore, we examined MEL-11 localization in a partial loss-of-function *let-502(sb106)* mutant, which does elongate. Although less dramatic compared with the strong allele *let-502(ca201)*, we again found higher levels of cytoplasmic MEL-11 in the in *let-502(sb106)* embryos compared with wild type (Fig. 7C,D). This suggests that the

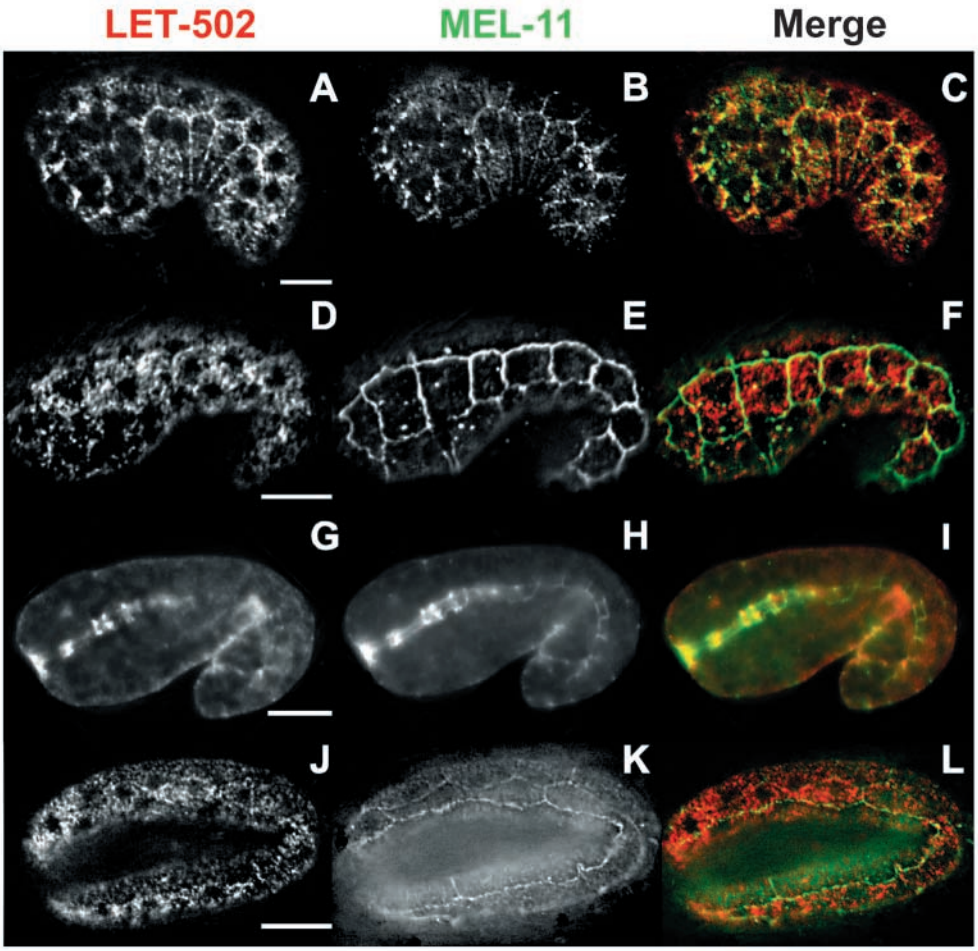

Fig. 5. LET-502 and MEL-11 immunolocalization in wild-type embryos. Embryos in the first column are stained with anti-LET-502, middle column with anti-MEL-11 and merged images are presented in the right column (LET-502 red, MEL-11 green). (A-C) 1.0- to 1.5-fold embryo showing extensive colocalization of LET-502 and MEL-11 in all epidermal cells. (D-F) Twofold embryo is shown at a plane corresponding to the epidermal cells where MEL-11 is restricted to epidermal cell boundaries while LET-502 remains cytoplasmic. (G-I) Twofold embryo at a plane corresponding to pharynx and intestine, where LET-502 and MEL-11 colocalized at adherens junctions. (J-L) Threefold embryo showed cytoplasmic LET-502, while MEL-11 showed punctate staining at the cell boundaries, with a limited amount reappearing in the cytoplasm (compare E and K). All images were deconvolved. Scale bars: 10 μm.

disappearance of the cytoplasmic MEL-11 pool, which occurs at the onset of elongation and which could potentially inhibit myosin activity, is at least partly dependent on *let-502(+)* activity. This is consistent with the antagonistic genetic interactions of *let-502* and *mel-11*.

Although the above evidence supports the model that LET-502 and MEL-11 regulate myosin activity to drive elongation, another (not mutually exclusive) model proposes that LET-502 and MEL-11 regulate anchoring of actin cables to the membranes of the lateral epidermal cells. Elongation-defective

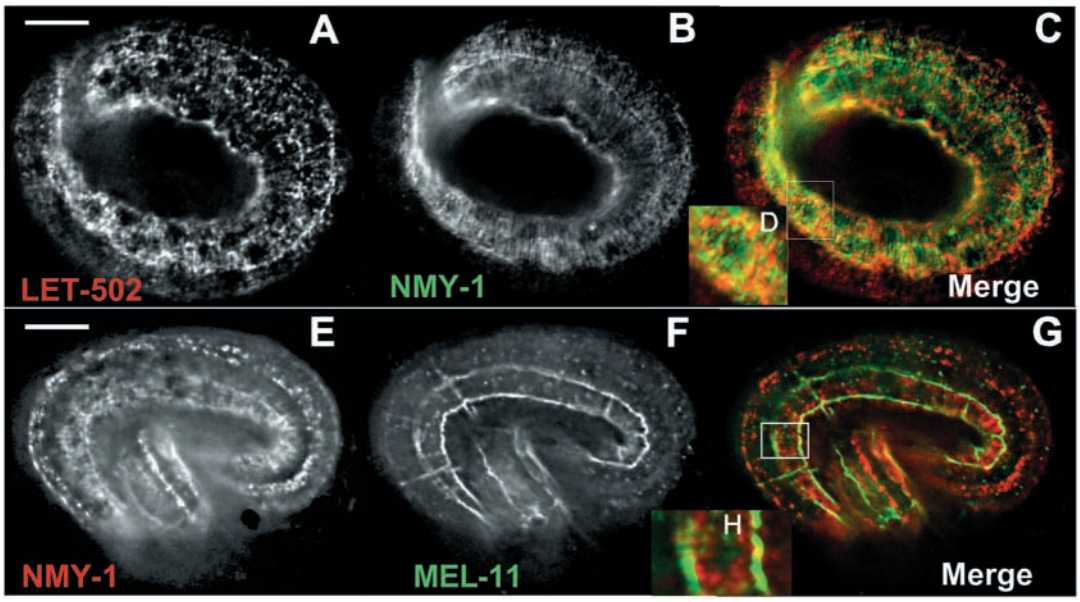

Fig. 6. LET-502, but not MEL-11, localizes near NMY-1. In elongating embryos, LET-502 (A) was interspersed with filamentous NMY-1 (B). Merged image is shown in C (LET-502 red, NMY-1 green). A magnified view of C is shown in D. MEL-11 was restricted to epidermal cell boundaries (F) away from NMY-1 (E), with a merged image shown in G (NMY-1 red, MEL-11 green). A magnified view is included in H. All images were deconvolved. Scale bars: 10 μm.

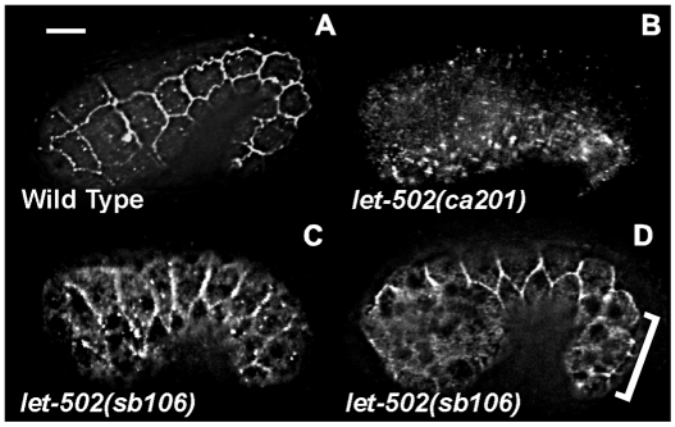

Fig. 7. MEL-11 is dependent on LET-502 for its localization. Although only low levels of cytoplasmic anti-MEL-11 staining was present in the lateral epidermal cells of wild type (A), higher cytoplasmic levels were present in *let-502(ca201)* (B), which arrests at the onset of elongation. *let-502(sb106)* embryos undergo elongation, albeit abnormally, and also show higher levels of cytoplasmic MEL-11 (C). The *let-502(sb106)* embryos in D is at a later stage than that in C, and again showed higher levels of cytoplasmic MEL-11 compared with wild type (A). The embryo in D presents a more ventral aspect; the posterior lateral epidermal cells indicated by the bracket were in the focal plane and show increased cytoplasmic MEL-11. All images were deconvolved. Scale bar: 10 μm.

phenotypes are observed in genes such as *sma-1* (β_H-spectrin), *spc-1* (α-spectrin), *hmr-1* (cadherin) and *hmp-1* and *hmp-2* (catenins), the products of which are required to tether actin filaments to the membranes of the lateral epidermal cells (Costa et al., 1998; McKeown et al., 1998; Norman and Moerman, 2002). We found that *spc-1* and *sma-1* are genetically epistatic with *mel-11*, suggesting that *mel-11* hypercontraction requires the anchoring of actin cables by these genes (Table 1). However, if LET-502 is involved in anchoring these cables, then we would expect high levels of LET-502 (a possible positive regulator of actin anchoring) and low levels of MEL-11 (a possible negative regulator of anchoring) at the membrane. However, we saw the exact opposite staining pattern (Fig. 5). As reported by Norman and Moerman (Norman and Moerman, 2002), we observed normal actin filaments in *let-502* and *mlc-4* mutants, as well as in *nmy-1(sb113)* and *mel-11(it26)* embryos (data not shown). Our results thus suggest that LET-502 and MEL-11 are not required to anchor actin filaments, but likely regulate the contraction of filaments. However, LET-502 and MEL-11 are present at the AJs of the pharynx and gut, and could be required for some aspect of AJ formation or function in these organs.

MEL-11 requires NMY-1 for membrane localization

Drosophila Zipper/nonmuscle myosin requires Spaghetti squash/rMLC for localization (Edwards and Kiehart, 1996; Jordan and Karess, 1997; Wheatley et al., 1995). We found that NMY-1 similarly failed to form filamentous-like structures in *mlc-4*-null mutant embryos, with NMY-1 collapsing into large foci (Fig. 8A).

As myosin is the target of MEL-11, we expected that MEL-11 localization might change in *nmy-1* and *mlc-4* mutants. However, *mlc-4* embryos displayed wild-type patterns of MEL-11 (Fig. 8B,C) and F-actin distribution (data not shown) (Norman and Moerman, 2002). We also examined *nmy-1(sb113); nmy-2(RNAi)* embryos, which lack all MHC and arrest at a similar stage to *mlc-4*. MEL-11 no longer localized to membranes (Fig. 8D-F). When MHC was partly eliminated using *nmy-1(sb113)*, membrane localization of MEL-11 was frequently decreased and occasionally was absent. An extreme case is shown in Fig. 8G-I, which may correspond to those rare *sb113* embryos where elongation failed. These results may

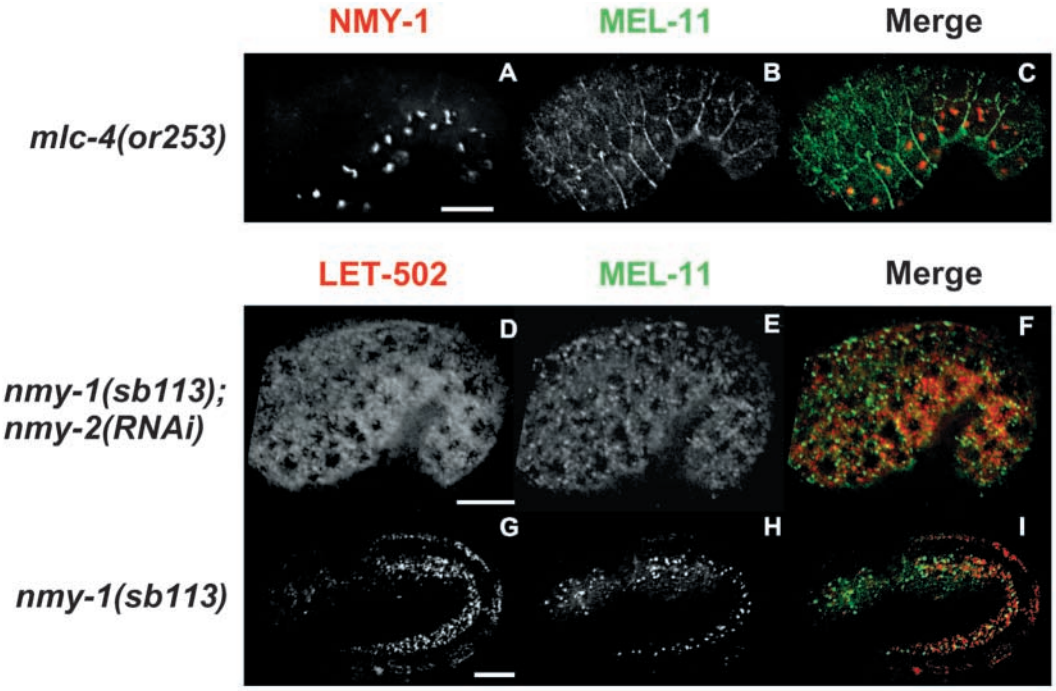

Fig. 8. NMY-1 and MEL-11 localization in myosin-depleted embryos. In *mlc-4* embryos, NMY-1 collapsed into large foci (A), but MEL-11 was unaffected (B). A merged image is shown in (C, NMY-1 red, MEL-11 green). However, although LET-502 appeared normal (D), MEL-11 was clearly disrupted in *nmy-1(sb113); nmy-1(RNAi)* embryos (E, merged image shown in F with LET-502 red, MEL-11 green) where it remained cytoplasmic in comparison to its membrane location in wild-type embryos of similar stages (e.g. Fig. 5E). MEL-11 membrane localization was decreased compared with the normal pattern of LET-502 (G), or as shown in this embryo (H), occasionally absent when total NMY was only partially depleted in *nmy-1(sb113)* (I, merged image, LET-502 red, MEL-11 green). Scale bar: 10 μm.

indicate that the LET-502 interaction that directs MEL-11 to the membrane likely requires MEL-11 binding to MHC.

Discussion

NMY-1 is a nonmuscle MHC partner for MLC-4 during elongation

Elongation of the *C. elegans* embryo occurs due to actin-mediated contractions within the lateral epidermal (seam) cells (Priess and Hirsh, 1986). We previously identified a pathway that regulates elongation that includes LET-502/ROK and MEL-11/MYPT (Piekny et al., 2000; Piekny and Mains, 2002; Wissmann et al., 1997; Wissmann et al., 1999). MEL-11 prevents contraction by dephosphorylating MLC-4/rMLC. LET-502 in turn inhibits MEL-11, releasing the block to elongation. We describe a new component of the pathway, NMY-1/MHC, identified by mutations that suppress *mel-11(–)* hypercontraction. Based on genetic and molecular analyses, NMY-1 is an MHC partner for MLC-4/rMLC. Fig. 9 models how NMY-1, LET-502 and MEL-11 regulate elongation. At the onset of morphogenesis, actin and NMY-1 each form filamentous-like structures that probably constitute the contractile apparatus that drives elongation (Fig. 4). Similar to MYPT during smooth muscle contraction (Shin et al., 2002), MEL-11 moves from the cytoplasm to the membrane, away from the contractile apparatus, when contraction begins (Figs 5 and 6). After elongation is complete, low levels of cytoplasmic MEL-11 reappear. This MEL-11 membrane sequesterization depends at least in part on *let-502* activity, consistent with LET-502 triggering elongation by MEL-11 inhibition (Fig. 7). Membrane localization was also disrupted when total NMY levels are reduced or eliminated, suggesting that the MEL-11/LET-502 interaction occurs on myosin (Fig. 8). Thus, the defective elongation seen in *nmy-1* mutants may not only stem from decreased amounts of MHC, but also from an inhibition of myosin activity by the increased levels of cytoplasmic MEL-11.

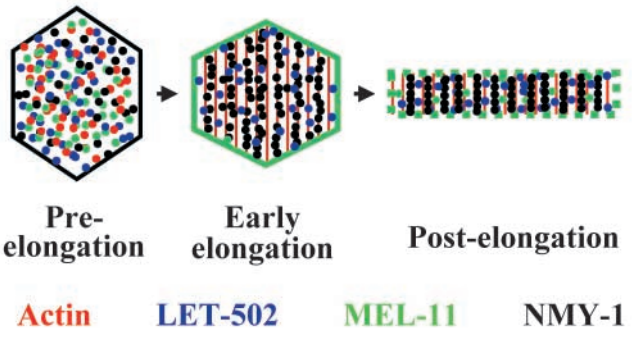

Fig. 9. A cartoon model demonstrating how actin, NMY-1, LET-502 and MEL-11 regulate elongation of lateral epidermal cells. Prior to elongation, actin (red) is disorganized and NMY-1 (black), LET-502 (blue) and MEL-11 (green) are present throughout the cell. In the early stages of elongation, actin filaments organize perpendicular to the direction of the future cell shape changes. NMY-1 begins to organize into filaments, where it could function as a motor to shorten actin filaments. LET-502 remains at high levels within the cell where it likely phosphorylates and thus sequesters MEL-11 to the membrane. By the end of elongation, NMY-1 forms perpendicular lines similar to actin. LET-502 remains associated with NMY-1 and MEL-11 loses its strong membrane localization and partially returns to the cytoplasm, where it could downregulate myosin activity.

In contrast to MEL-11 membrane sequesterization during elongation, LET-502 is interspersed with the myosin filaments (Fig. 6). In addition to triggering contraction by MYPT inhibition, ROK can directly phosphorylate rMLC in some in vitro systems (Amano et al., 1996). The localization of LET-502 with the NMY-1 filaments is consistent with this possibility.

Similar to what is seen in *Drosophila* (Edwards and Kiehart, 1996; Jordan and Karess, 1997; Wheatley et al., 1995), NMY-1 fails to form filaments in *mlc-4* mutants but instead forms discrete foci, suggesting that MLC-4 is required for the proper myosin organization. In higher eukaryotes, rMLC is not required for MHC to assemble into contractile units, but rMLC phosphorylation establishes contacts between myosin and actin filaments (Trybus, 1996). Perhaps actin association is required to assemble NMY-1 into the ordered arrays we observe in *C. elegans* embryos. In the absence of *mlc-4*/rMLC, NMY-1 assembly is more random, forming the large foci rather than parallel arrays.

In addition to a role for LET-502 and MEL-11 in regulating the contraction of actin, an alternative model would suggest that like their mammalian homologs in focal adhesion formation, LET-502 and MEL-11 could regulate the attachment of actin cables at the apical surfaces of lateral epidermal cells. The *C. elegans* α and β_H-spectrin genes, *spc-1* and *sma-1*, respectively, display elongation defects not unlike those seen in *let-502* or *mlc-4* mutants (McKeown et al., 1998; Norman and Moerman, 2002), and we observed that *spc-1* and *sma-1* are epistatic to *mel-11* hypercontraction (Table 1). However, Norman and Moerman (Norman and Moerman, 2002) showed that the actin cables were not disrupted in *let-502* and *mlc-4* mutants, and we found that this was also the case for *mel-11* and *nmy-1*. Moreover, the immunolocalization patterns for LET-502 and MEL-11 are opposite to that predicted by the actin anchoring model: LET-502, which would be predicted to tether actin to the membrane, remains cytoplasmic, while MEL-11, which would release the cables, is found at the membrane. Therefore, these results support a role for the LET-502/MEL-11 pathway in regulating the contraction of actin/myosin rather than anchoring of actin filaments.

nmy-2 is partially redundant with *nmy-1* during elongation

Our analysis of *nmy-1* suggests that it functions redundantly with another gene during embryonic elongation. The *nmy-1* null phenotype, a mis-shapen adult, is much less severe than expected if it were the only MHC to regulate this process as *mlc-4*, the only rMLC known to function during elongation, displays arrest as unelongated L1 larva (Shelton et al., 1999). We demonstrated that a second MHC gene, *nmy-2*, functions redundantly with *nmy-1*. *nmy-2(RNAi)* disrupts AP polarity and cytokinesis in the early embryo (Cuenca et al., 2003; Guo and Kemphues, 1996), which prevented examining *nmy-2* function later in embryogenesis. However, we found that NMY-2 is present in epidermal cells at the onset of elongation, where it likely assembles into filamentous structures similar to NMY-1. Furthermore, *nmy-2(weak RNAi)*; *nmy-1* double mutants displayed elongation-defective phenotypes similar to *mlc-4* that were not seen for either *nmy-2(weak RNAi)* or *nmy-1* alone (Table 3). Therefore, we have uncovered a role for *nmy-2* in elongation.

To summarize, we have isolated a new component of the *let-*

502/mel-11 pathway, *nmy-1*, which encodes a nonmuscle MHC that functions with *mlc-4*/rMLC to regulate the contractile process of embryonic elongation. *nmy-1* functions redundantly with a second nonmuscle MHC gene, *nmy-2*. Together the two MHCs ensure the successful elongation of embryos into the characteristic long, thin worm.

We thank M. Walsh, W. Brook and J. McGhee for advice and comments on the manuscript, S. McWilliams for technical assistance, K. Kemphues for NMY-2 antibodies, K. Norman and D. Moerman for *spc-1*, and M. Glotzer for advice and reagents. Some strains were obtained from the *Caenorhabditis* Genetics Center, funded by the National Institutes of Health National Center for Research Resources. This work was supported by Canadian Institutes for Health Research and Alberta Heritage Foundation for Medical Research grants to P.E.M.

References

Amano, M., Ito, M., Kimura, K., Fukata, Y., Chihara, K., Nakano, T., Matsuura, Y. and Kaibuchi, K. (1996). Phosphorylation and Activation of Myosin by Rho-associated Kinase (Rho-kinase). *J. Biol. Chem.* **271**, 20246-20249.

Brenner, S. (1974). The genetics of *Caenorhabditis elegans*. *Genetics* **77**, 71-94.

Chin-Sang, I. D. and Chisholm, A. D. (2000). Form of the worm: genetics of epidermal morphogenesis in *C. elegans*. *Trends Genet.* **16**, 544-551.

Costa, M., Raich, W., Agbunag, C., Leung, B., Hardin, J. and Priess, J. R. (1998). A putative catenin-cadherin system mediates morphogenesis of the *Caenorhabditis elegans* embryo. *J. Cell Biol.* **141**, 297-308.

Cuenca, A. A., Schetter, A., Aceto, D., Kemphues, K. and Seydoux, G. (2003). Polarization of the *C. elegans* zygote proceeds via distinct establishment and maintenance phases. *Development* **130**, 1255-1265.

Edgley, M., Baillie, D. L., Riddle, D. L. and Rose, A. M. (1995). Genetic balancers. In *Caenorhabditis elegans*: *Modern Biological Analysis of an Organism* (ed. H. F. Epstein and D. C. Shakes), pp. 147-184. San Diego: Academic Press.

Edwards, K. A. and Kiehart, D. P. (1996). *Drosophila* nonmuscle myosin II has multiple essential roles in imaginal disc and egg chamber morphogenesis. *Development* **122**, 1499-1511.

Fire, A., Xu, S., Montgomery, M. K., Kosatas, S. A., Driver, S. E. and Mello, C. C. (1998). Potent and specific genetic interference by double-stranded RNA in *Caenorhabditis elegans*. *Nature* **391**, 806-811.

Fraser, A. G., Kamath, R. S., Zipperlen, P., Martinez-Campos, M., Sohrmann, M. and Ahringer, J. (2000). Functional genomic analysis of *C. elegans* chromosome I by systematic RNA interference. *Nature* **408**, 325-330.

Guo, S. and Kemphues, K. J. (1996). A non-muscle myosin required for embryonic polarity in *Caenorhabditis elegans*. *Nature* **382**, 455-458.

Hill, A. A., Hunter, C. P., Tsung, B. T., Tucker-Kellogg, G. and Brown, E. L. (2000). Genomic analysis of gene expression in *C. elegans*. *Science* **290**, 809-812.

Hodgkin, J. (1997) Genetics. In *C. elegans II* (ed. D. L. Riddle, T. Blumenthal, B. J. Meyer and J. R. Priess), pp. 881-1047. New York: Cold Spring Harbor Press.

Horvitz, H. R., Brenner, S., Hodgkin, J. and Herman, R. K. (1979). A uniform genetic nomenclature for the nematode *Caenorhabditis elegans*. *Mol. Gen. Genet.* **175**, 129-133.

Horvitz, H. R. and Sulston, J. E. (1980). Isolation and genetic characterization of cell-lineage mutants of the nematode *Caenorhabditis elegans*. *Genetics* **96**, 435-454.

Jordan, P. and Karess, R. (1997). Myosin light chain-activating phosphorylation sites are required for oogenesis in *Drosophila*. *J. Cell Biol.* **139**, 1805-1819.

Kaibuchi, K., Kuroda, S. and Amano, M. (1999). Regulation of the cytoskeleton and cell adhesion by the Rho family GTPases in mammalian cells. *Annu. Rev. Biochem.* **68**, 459-486.

Kamath, R. S., Fraser, A. G., Dong, Y., Poulin, G., Durbin, R., Gotta, M., Kanapin, A., le Bot, N., Moreno, S., Sohrmann, M. et al. (2003). Systematic functional analysis of the *Caenorhabditis elegans* genome using RNAi. *Nature* **421**, 232-237.

Mains, P. E., Sulston, I. A. and Wood, W. B. (1990). Dominant maternal-effect mutations causing embryonic lethality in *Caenorhabditis elegans*. *Genetics* **125**, 351-369.

Mansfield, S. G., al-Shirawi, D. Y., Ketchum, A. S., Newbern, E. C. and Kiehart, D. P. (1996). Molecular organization and alternative splicing in zipper, the gene that encodes the *Drosophila* non-muscle myosin II heavy chain. *J. Mol. Biol.* **255**, 98-109.

McKeown, C., Praitis, V. and Austin, J. (1998). *sma-1* encodes a β_H-spectrin homolog required for *Caenorhabditis elegans* morphogenesis. *Development* **125**, 2087-2098.

Mizuno, T., Tsutsui, K. and Nishida, Y. (2002). *Drosophila* myosin phosphatase and its role in dorsal closure. *Development* **129**, 1215-1223.

Norman, K. R. and Moerman, D. G. (2002). α spectrin is essential for morphogenesis and body wall muscle formation in *Caenorhabditis elegans*. *J. Cell Biol.* **157**, 665-667.

Pfitzer, G. (2001). Signal transduction in smooth muscle. Invited review: regulation of myosin phosphorylation in smooth muscle. *J. Appl. Physiol.* **91**, 497-503.

Philips, C. L., Yamakawa, K. and Adelstein, R. S. (1995). Cloning of the cDNA encoding human nonmuscle myosin heavy chain-B and analysis of human tissues with isoform-specific antibodies. *J. Muscle Res. Cell Motil.* **16**, 379-389.

Piekny, A. J., Wissmann, A. and Mains, P. E. (2000). Embryonic morphogenesis in *Caenorhabditis elegans* integrates the activity of LET-502 Rho-binding kinase, MEL-11 myosin phosphatase, DAF-2 insulin receptor and FEM-2 PP2c phosphatase. *Genetics* **156**, 1671-1689.

Piekny, A. J. and Mains, P. E. (2002). Rho-binding kinase (LET-502) and myosin phosphatase (MEL-11) regulate cytokinesis in the early *Caenorhabditis elegans* embryo. *J. Cell Sci.* **115**, 2271-2282.

Priess, J. R. and Hirsh, D. I. (1986). *Caenorhabditis elegans* morphogenesis: the role of the cytoskeleton in elongation of the embryo. *Dev. Biol.* **117**, 156-173.

Shelton, C. A., Carter, J. C., Ellis, G. C. and Bowerman, B. (1999). The nonmuscle myosin regulatory light chain gene *mlc-4* is required for cytokinesis, anterior-posterior polarity, and body morphology during *Caenorhabditis elegans* embryogenesis. *J. Cell Biol.* **146**, 439-451.

Shin, H. M., Je, H. D., Gallant, C., Tao, T. C., Hartshorne, D. J., Ito, M. and Morgan, K. G. (2002). Differential association and localization of myosin phosphatase subunits during agonist-induced signal transduction in smooth muscle. *Circ. Res.* **90**, 546-553.

Simske, J. S. and Hardin, J. (2001). Getting into shape: epidermal morphogenesis in *Caenorhabditis elegans* embryos. *BioEssays* **23**, 12-23.

Somlyo, A. P. and Somlyo, A. V. (2000). Signal transduction by G-proteins, Rho-kinase and protein phosphatase to smooth muscle and non-muscle myosin II. *J. Physiol.* **522**, 177-185.

Tabara, H., Sarkissian, M., Kelly, W. G., Fleenor, J., Grishok, A., Timmons, L., Fire, A. and Mello, C. C. (1999). The *rde-1* gene, RNA interference, and transposon silencing in *C. elegans*. *Cell* **99**, 123-132.

Tan, C., Stronach, B. and Perrimon, N. (2003). Roles of myosin phosphatase during *Drosophila* development. *Development* **130**, 671-681.

Trybus, K. M. (1996). Myosin regulation and assembly. In *Biochemistry of Smooth Muscle Contraction* (ed. M. Barany), pp. 37-45. San Diego: Academic Press.

Wheatley, S., Kulkarni, S. and Karess, R. (1995). *Drosophila* nonmuscle myosin II is required for rapid cytoplasmic transport during oogenesis and for axial nuclear migration in early embryos. *Development* **121**, 1937-1946.

Wicks, S. R., Yeh, R. T., Gish, W. R., Waterston, R. H. and Plasterk, R. H. (2001). Rapid gene mapping in *Caenorhabditis elegans* using a high density polymorphism map. *Nat. Genet.* **28**, 160-164.

Winter, C. G., Wang, B., Ballew, A., Royou, A., Karess, R., Axelrod, J. D. and Luo, L. (2001). *Drosophila* Rho-associated kinase (Drok) links Frizzled-mediated planar cell polarity signaling to the actin cytoskeleton. *Cell* **105**, 81-91.

Wissmann, A., Ingles, J., McGhee, J. D. and Mains, P. E. (1997). *Caenorhabditis elegans* LET-502 is related to Rho-binding kinases and human myotonic dystrophy kinase and interacts genetically with a homolog of the regulatory subunit of smooth muscle myosin phosphatase to affect cell shape. *Genes Dev.* **11**, 409-422.

Wissmann, A., Ingles, J. and Mains, P. E. (1999). The *Caenorhabditis elegans mel-11* myosin phosphatase regulatory subunit affects tissue contraction in the somatic gonad and the embryonic epidermis and genetically interacts with the Rac signaling pathway. *Dev. Biol.* **209**, 111-127.

Young, P. E., Richman, A. M., Ketchum, A. S. and Kiehart, D. P. (1993). Morphogenesis in *Drosophila* requires nonmuscle myosin heavy chain function. *Genes Dev.* **7**, 29-41.